THE JOURNAL OF BIOLOGICAL CHEMISTRY VOL. 289, NO. 16, pp. 11367–11373, April 18, 2014

Phosphorylation Regulates the p31^{Comet}-Mitotic Arrest-deficient 2 (Mad2) Interaction to Promote Spindle Assembly Checkpoint (SAC) Activity*

Received for publication, September 23, 2013, and in revised form, March 3, 2014 Published, JBC Papers in Press, March 4, 2014, DOI 10.1074/jbc.M113.520841

Dipali A. Date, Amy C. Burrows, and Matthew K. Summers[1]

From the Department of Cancer Biology, Lerner Research Institute, Cleveland, Ohio 44195

Background: p31^{Comet} antagonizes the SAC effector Mad2 to promote mitotic progression.
Results: p31^{Comet} phosphorylation modulates binding to Mad2.
Conclusion: Phosphorylation attenuates binding of Mad2 by p31^{Comet} to promote SAC activity.
Significance: Our study provides the first description of p31^{Comet} regulation and new insight into the control of SAC activity.

The spindle assembly checkpoint (SAC) ensures the faithful segregation of the genome during mitosis by ensuring that sister chromosomes form bipolar attachments with microtubules of the mitotic spindle. p31^{Comet} is an antagonist of the SAC effector Mad2 and promotes silencing of the SAC and mitotic progression. However, p31^{Comet} interacts with Mad2 throughout the cell cycle. We show that p31^{Comet} binds Mad2 solely in an inhibitory manner. We demonstrate that attenuating the affinity of p31^{Comet} for Mad2 by phosphorylation promotes SAC activity in mitosis. Specifically, phosphorylation of Ser-102 weakens p31^{Comet}-Mad2 binding and enhances p31^{Comet}-mediated bypass of the SAC. Our results provide the first evidence for regulation of p31^{Comet} and demonstrate a previously unknown event controlling SAC activity.

The spindle assembly checkpoint (SAC)[2] is an evolutionarily conserved and essential surveillance mechanism that ensures that chromosome segregation during mitosis proceeds with high fidelity. The SAC monitors the attachment of chromosomes to microtubules of the mitotic spindle and mediates inhibition of the anaphase-promoting complex (APC) ubiquitin ligase. SAC activity persists until each kinetochore of the sister chromosome pairs have achieved attachment to microtubules emanating form opposite poles of the spindle and are under tension. Kinetochores that are unattached or that are not under tension recruit SAC components that ultimately lead to the activation of the effector molecules Mad2 and BubR1. Upon activation, Mad2 and BubR1, along with Bub3, bind the APC activator/adapter protein Cdc20 to form the mitotic checkpoint complex (MCC), resulting in inhibition of APC^{Cdc20} activity (1).

The Mad2 protein exists in two conformations: closed C-Mad2 (active) and open O-Mad2 (inactive) (2–10). Activation of the checkpoint recruits the C-Mad2/Mad1 heterodimer to the kinetochore. C-Mad2, in this complex, then dimerizes with cytoplasmic Mad2 to catalyze the formation of additional C-Mad2 molecules that directly bind Cdc20. Binding of Cdc20 by Mad2 primes it for binding by BubR1/Bub3 to form the MCC and prevent mitotic progression (11).

Once all kinetochores have achieved proper attachment, the checkpoint is satisfied and mitotic progression resumes. Recovery from SAC activity occurs in two steps: termination of MCC formation and disassembly of preexisting MCCs. p31^{Comet} is a key factor in the recovery of cells from SAC activity (12–16). p31^{Comet} specifically binds C-Mad2 via the same binding interface as O-Mad2 (9, 12, 17, 18). p31^{Comet} silences SAC activity *in vitro* and *in vivo* in a manner that requires this interaction with Mad2 (18). p31^{Comet} interacts with C-Mad2 in both the MCC and the C-Mad2·Mad1 complex and has been demonstrated to antagonize both (9, 12, 17–19).

We and others (20–23) have shown that APC^{Cdc20} remains inhibited in extracts generated from SAC-active cells, despite the presence of p31^{Comet} in these extracts. These data suggest that p31^{Comet} is activated upon satisfaction of the SAC to facilitate recovery from the checkpoint. Consistent with this idea, the presence of p31^{Comet} in Cdc20 immunocomplexes has been shown to increase upon release from nocodazole (*i.e.* during SAC recovery) (12). However, p31^{Comet} and Mad2 interact throughout the cell cycle, including early mitosis when the SAC is active (15, 16, 19).

We have examined the mechanism that permits SAC activity despite the interaction of a key effector molecule with its antagonist. We show that p31^{Comet} interacts with Mad2 solely as an inhibitor. Moreover, we demonstrate that although the two proteins can be found in complex through out the cell cycle, phosphorylation of p31^{Comet} during mitosis weakens the interaction with Mad2, as judged by competition assays, to allow SAC activity.

EXPERIMENTAL PROCEDURES

Cell Culture—HeLa and HCT116 cells were obtained from ATCC and maintained in DMEM supplemented with 10% FBS.

* This work was supported by seed funds form the Lerner Research Institute, American Cancer Society Grant IRG-91-022-15, and pilot funds from the Ohio Cancer Research Associates (to M. K. S.).
[1] To whom correspondence should be addressed: Dept. of Cancer Biology, Lerner Research Inst., 9500 Euclid Ave., NB40, Cleveland, OH 44195. Tel.: 216-445-2555; E-mail: summerm@ccf.org.
[2] The abbreviations used are: SAC, spindle assembly checkpoint; APC, anaphase-promoting complex; MCC, mitotic checkpoint complex; C-Mad2, closed Mad2; O-Mad2, open Mad2.

Cells were synchronized as described (20). Nocodazole was added 5 h after release from thymidine. Cells were transfected with Transit-LT1 (Mirus) or RNAiMax (Invitrogen) per manufacturer's instructions. Where indicated, cells were treated with 100 ng/ml nocodazole. HeLa Flp-In T-Rex cells were a gift of Dr. Stephen Taylor (15). Isogenic p31^{Comet} WT and S102A cell lines were generated with the use of pGLAP2 as described (24).

Antibodies—Anti-Myc (9E10) was produced at the Lerner Research Insitute. Commercial antibodies were as follows: cyclin B (GNS1), p31^{Comet} (4RE23), and Mad2 (107–276-3) from Santa Cruz Biotechnology; actin (AC-15), FLAG (M2), and p31^{Comet} (4G11) from Sigma; p31^{Comet} (EPR9584) from Abcam.

Plasmids and Recombinant Proteins—A gateway-compatible open reading frame for p31^{Comet} was obtained from Origene. Subcloning was performed using LR clonase to transfer the ORF into pCS2, pGLAP2, and pGex6P1-derived destination vectors. Mutagenesis was performed using the QuikChange mutagenesis strategy. His$_6$-p31^{Comet} Δ35 produced as described (20).

Western Blotting, Immunoprecipitation, and Phos-tag Analysis—Cell extracts were generated in EBC buffer (50 mM Tris (pH 8.0), 120 mM NaCl, 0.5% Nonidet P-40, 1 mM DTT, 25 mM β-glycerophosphate, 5 mM NaF, 1 mM $NaVO_4$, and leupeptin, pepstatin, and chymotrypsin, each at 10 μg/ml. For immunoprecipitation, equal amounts of cell lysates were incubated with the indicated antibodies for 2–12 h and washed in EBC buffer, including inhibitors. Immunoprecipitation samples or equal amounts of whole cell lysates were resolved by SDS-PAGE. For analysis of phosphorylation, proteins were resolved on 8% SDS-PAGE gels incorporating 40 μM Phos-tag reagent (Wako) and 80 μM $MnCl_2$. Proteins were transferred to PVDF membranes (Millipore) probed with the indicated antibodies and visualized with the LI-COR Odyssey near infrared imaging system.

In Vitro Phosphorylation and Mass Spectrometry—HCT116 cells were synchronized and harvested in mitosis after a thymidine-nocodazole block or in late M/early G_1, 2 h after release from a thymidine-nocodazole block. Extracts were then prepared by resuspension in extract buffer (20 mM Tris-HCl, pH 7.2, 2 mM DTT, 0.25 mM EDTA, 5 mM KCl, 5 mM $MgCl_2$) followed by two rounds of freeze-thaw and passage through a needle. Extracts were supplemented with ATP and an energy-regenerating system. Mitotic extracts were supplemented with non-destructible cyclin B1 and MG132 to maintain the mitotic state. GST-p31^{Comet} was then incubated in extract for 1 h at 30 °C and then captured on glutathione-agarose. After washing, the proteins were resolved on Phos-tag gels as above and visualized with Gelcode Blue (Pierce). Protein bands were digested with trypsin, extracted in 50% acetonitrile and 5% formic acid. After evaporation, peptides were resuspended in 1% acetic acid and analyzed on a Finnigan LTQ-Obitrap Elite hybrid mass spectrometer system. The HPLC column was a Dionex (15 cm, × 75 μm inner diameter) Acclaim Pepmap C18 (2 μm) 100 Å reversed phase capillary chromatography column.

Live Cell Microscopy—Isogenic HeLa cell lines were plated in 24-well dishes and synchronized as above. Expression of p31^{Comet} proteins was induced after release from thymidine. Eight hours post-release, nocodazole was added, and cells were transferred to Leica DMIRB inverted microscope equipped with a Roper Scientific CoolSNAP HQ Cooled CCD camera (Roper Scientific, Tucson, AZ), temperature controller (37 °C) and CO_2 (5%) incubation chamber (Leica Microsystems GmbH), and a PeCon incubator (PeCon GmbH, Erbach, Germany) controlled by MetaMorph Software (Molecular Devices, Downingtown, PA). Images of multiple fields per well were collected at 10-min intervals and analyzed using ImageJ and Photoshop.

Statistical Analysis—One-way analysis of variance with Bonferroni post tests were performed using GraphPad Prism.

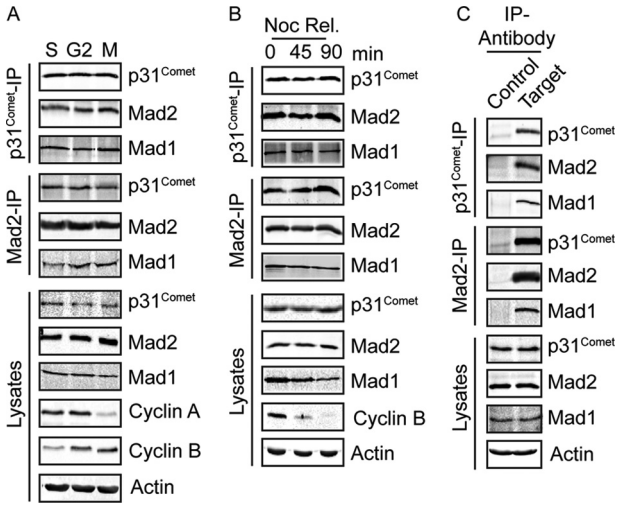

FIGURE 1. **p31^{Comet} and Mad2 interact throughout the cell cycle.** *A*, HCT116 cells were synchronized by a double thymidine block and released into nocodazole (*Noc*)-containing medium. Cells in S, G_2, and M phases were harvested at 2, 8, and 14 h, respectively. Lysates and p31^{Comet} or Mad2 immunoprecipitates (*IP*) were resolved by SDS-PAGE and blotted with the indicated antibodies. Cyclins A and B were probed as markers for the indicated cell cycle phases. *B*, HCT116 cells were synchronized in mitosis by thymidine-nocodazole block and released (Rel.) into fresh medium. Cells harvested at the indicated time points were resolved as in *A*. Cyclin B levels were probed to monitor the efficiency of mitotic exit. *C*, asynchronous lysates were immunoprecipitated with control IgGs or the indicated antibodies and analyzed as described in *A*.

RESULTS

p31^{Comet} and Mad2 Interact throughout the Cell Cycle—APC^{Cdc20} remains inhibited by the MCC in extracts derived from mitotic, SAC-active cells, despite the presence of p31^{Comet} in these extracts (20–22). In addition, association of p31^{Comet} with Cdc20 increases during release from a nocodazole block (12). Together, these data suggest that an activating event promotes the interaction of p31^{Comet} with Mad2 followed by subsequent silencing of SAC activity. To identify this event, we sought to confirm that the binding of p31^{Comet} to Mad2 follows this model, that is, that p31^{Comet} binds and antagonizes Mad2 during mitotic exit. To analyze the interaction of p31^{Comet} and Mad2, we examined both p31^{Comet} and Mad2 immunocomplexes for the presence of the interacting partner as well as the Mad2 interactor Mad1. Unexpectedly, we found that p31^{Comet} interacted with Mad2 as well as the Mad2 heterodimeric partner Mad1 at all stages of the cell cycle (Fig. 1*A*). Notably, p31^{Comet} associates with Mad2 and Mad1 in cells arrested in

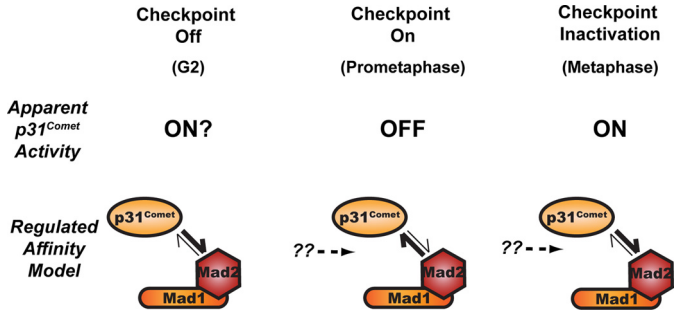

FIGURE 2. **Models of p31^{Comet}-Mad2 interaction.** *Apparent p31^{Comet} Activity*, during G_2/interphase, p31^{Comet} may actively prevent the generation of low levels of C-Mad2 (15). p31^{Comet} activity is low during prometaphase to allow SAC activity. Upon attachment of all chromosomes at metaphase, p31^{Comet} binds active Mad2, preventing further Mad2 activation and silences the SAC. *Regulated Affinity Model*, our proposed model. The affinity of p31^{Comet} for Mad2 is diminished in early mitosis, due to post-translational modification(s), to promote SAC activity. Loss of early mitotic modifications and/or late mitosis-specific modifications enhance p31^{Comet} affinity for Mad2 to promote SAC silencing.

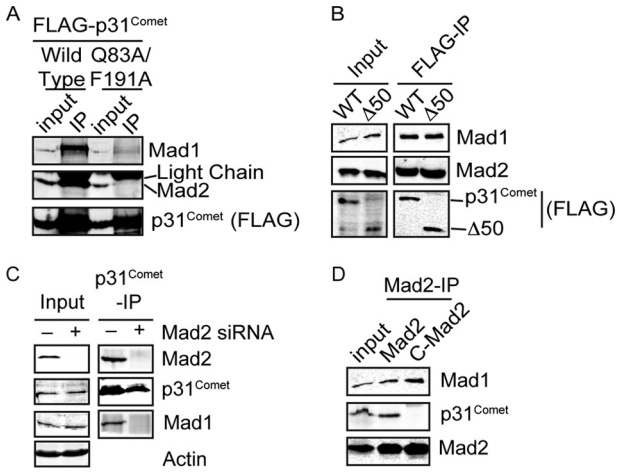

FIGURE 3. **p31^{Comet} only binds Mad2 as an inhibitor.** *A*, HeLa cells were transfected with FLAG-tagged p31^{Comet} or the Mad2-binding mutant Q83A/F191A. Lysates and FLAG-immunoprecipitates (*IP*) were probed for the presence of Mad2 and Mad1. *B*, cells were transfected with FLAG-p31^{Comet} or a mutant lacking the N-terminal 50 residues (Δ50) and analyzed as described in *A*. *C*, cells were transfected with siRNAs targeting Mad2. Lysates and p31^{Comet}-IPs were analyzed as described in *A*. *D*, cell lysates were immunoprecipitated with antibodies recognizing total Mad2 or C-Mad2 and probed for the presence of Mad1 and p31^{Comet}.

mitosis by treatment with nocodazole, in which the SAC is maximally active and the interaction does not increase upon mitotic exit (Fig. 1, *A* and *B*). Several recent reports have confirmed our findings (15, 16, 19). These data pose a critical question: how does a cell mount a SAC-mediated mitotic arrest, whereas the critical SAC effector Mad2 is readily found in complex with its inhibitor p31^{Comet}?

p31^{Comet} Associates with Mad2 via a Single Interface—Analysis of the p31^{Comet} ΔN35-C-Mad2 crystal structure demonstrated that p31^{Comet} and O-Mad2 bind C-Mad2 via the same interface (18). Given this knowledge, the function of p31^{Comet}, and the interaction of p31^{Comet} with Mad2 throughout the cell cycle, we propose a model for the regulated inhibition of Mad2 by p31^{Comet} (Fig. 2). This model assumes that p31^{Comet} interacts with the C-Mad2:Mad1 heterodimer solely via the O-Mad2 binding interface of C-Mad2. To confirm the validity of this assumption, we asked whether the p31^{Comet} Q83A/F191A mutant was capable of binding to the C-Mad2:Mad1 heterodimer. Consistent with its inability to interact with C-Mad2, p31^{Comet} Q83A/F191A did not co-precipitate Mad1 (Fig. 3*A*). However, as no other direct p31^{Comet}-interacting proteins are known, it remained possible that the Q83A/F191A mutant is deficient in interactions that are independent of the O-Mad2 interface. Given the crystal structure data, we reasoned that such additional p31^{Comet}-Mad2 interactions would be mediated by the N terminus of p31^{Comet}, which is not present in the structure. p31^{Comet} deleted for the N-terminal 50 amino acids (Δ50) showed no defect in interacting with Mad2 or Mad1 (Fig. 3*B*). To exclude the possibility that the interaction with the C-Mad2:Mad1 heterodimer is mediated by a p31^{Comet}-Mad1 interaction not predicted by structural modeling, we determined that p31^{Comet} is not able to interact with Mad1 in the absence of Mad2 (Fig. 3*C*). Finally, we confirmed that immunoprecipitation of Mad2 using an antibody that specifically binds C-Mad2 via the O-Mad2/p31^{Comet} binding surface (see Ref. 16) does not co-precipitate p31^{Comet} as would be expected if an additional binding interface exists (Fig. 3*D*). Taken together, these data indicate that p31^{Comet} interacts with C-Mad2 and the C-Mad2:Mad1 heterodimer solely via the O-Mad2 binding interface. We conclude that p31^{Comet} associates with Mad2 in an inhibitory manner throughout the cell cycle.

The p31^{Comet}-Mad2 Interaction Is Weakened in Early Mitosis—We next tested our model, which predicts that the interaction of p31^{Comet} with Mad2 is weakened in mitosis (Fig. 2). We utilized an *in vitro* capture-chase assay. Recombinant GST-Mad2 bound to glutathione-agarose beads was incubated with extracts from cells that were SAC-active (nocodazole-arrested) or SAC-inactive (late mitotic/early G_1, nocodazole-released). We then tested the relative strength of p31^{Comet}-Mad2 binding by incubating the bead-bound complexes with increasing amounts of a recombinant p31^{Comet} with the N-terminal 35 amino acids deleted, p31^{Comet}Δ35. After washing, we probed the bound complexes for the presence of the full-length, captured p31^{Comet} with an N-terminal specific-antibody. As predicted by model 3, p31^{Comet} captured from mitotic extracts was more readily displaced from Mad2 than the p31^{Comet} from SAC-inactive extracts (Fig. 4*A*). The altered p31^{Comet} affinity depicted in Fig. 2 is the likely result of a post-translational modification. We therefore tested whether phosphorylation affected the affinity of p31^{Comet} for Mad2. We determined that p31^{Comet} is phosphorylated in mitosis by comparing the migration of p31^{Comet} in extracts of S, G_2, or mitosis on Phos-tag gels (25). These analyses indicated that a substantial portion of p31^{Comet} is phosphorylated during mitosis as evidenced by diminished electrophoretic migration (Fig. 4*B*). We confirmed that this altered mobility was indeed due to phosphorylation by treating mitotic lysates with λ-phosphatase prior to Phos-tag electrophoresis. Phophatase treatment resulted in a loss of the slower migrating forms of p31^{Comet}, confirming that p31^{Comet} is phosphorylated in mitosis (Fig. 4*C*).

To further determine that phosphorylation weakened the interaction between p31^{Comet} and Mad2, we utilized Phos-tag to analyze capture-chase assays similar to those above. To more closely recapitulate the physiological competition between

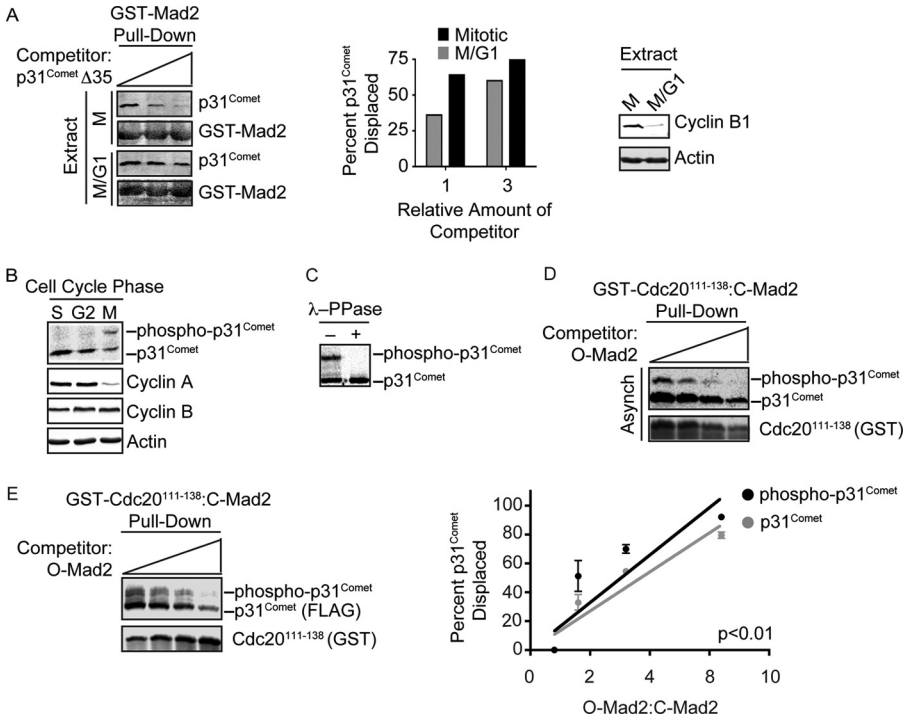

FIGURE 4. **Phosphorylation of p31^{Comet} weakens the interaction with Mad2 during mitosis.** *A*, *left panel*, p31^{Comet} was captured by recombinant Mad2 from extracts of nocodazole-arrested (*M*) or nocodazole-released (M/G_1) cells. Mad2-p31^{Comet} complexes were incubated with increasing amounts of recombinant p31^{Comet} Δ35 (N-terminal deletion) and retention of cellular p31^{Comet} was determined. *Middle panel*, quantification of the percent of captured p31^{Comet} that was displaced by Δ35. *Right panel*, cyclin B was probed in the same extracts to confirm mitotic status. *B*, HCT116 cells were synchronized as in 1A and lysates were resolved by Phos-tag SDS-PAGE to examine the phosphorylation status of p31^{Comet}. *C*, mitotic lysates were treated with or without λ-phosphatase and resolved by Phos-tag SDS-PAGE. *D*, p31^{Comet} was captured from asynchronous lysates by C-Mad2 in complex with GST-Cdc20$^{111-138}$. The relative strength of the interaction was tested by challenge with purified Mad2 (predominantly O-Mad2). Bound proteins were resolved by Phos-tag SDS-PAGE. *E*, FLAG-p31^{Comet} was phosphorylated in mitotic extract and then captured, challenged, and analyzed as described in *D*. *Right panel*, the mean and S.E. for the percent of p31^{Comet} displaced by increasing amounts of Mad2 was quantified ($n = 3$). The effect of phosphorylation on displacement of p31^{Comet} by Mad2 was analyzed by linear regression.

p31^{Comet} and O-Mad2 (or other C-Mad2 binding partners, *e.g.* BubR1) for C-Mad2, we captured p31^{Comet} from extract with C-Mad2 bound to the Mad2-binding region of Cdc20 (GST-Cdc20$^{111-138}$) and then challenged binding with the monomeric Mad2 (O-Mad2) (5, 17). We first captured endogenous p31^{Comet} from asynchronous extracts, which contained a minor but readily detectable mitotic phosphorylated form. When challenged with increasing molar ratio of O-Mad/C-Mad2, the phosphorylated form was lost more readily (Fig. 4*D*). To more closely examine the situation in mitosis, we phosphorylated a FLAG-p31^{Comet} in mitotic extracts and allowed a molar excess of this protein to bind the GST-Cdc20$^{111-138}$ and then performed the chase assays as above. The phosphorylated form was more readily displaced once the O-Mad2/C-Mad2 increased over 1:1 (Fig. 4*E*). These data indicate that phosphorylation lowers the affinity of p31^{Comet} for Mad2 during mitosis.

Phosphorylation of Ser-102 Regulates the Mad2 Interaction—We next sought to identify the mitosis-specific phosphorylation event(s) that mediate the weakened binding to Mad2. To facilitate the purification of p31^{Comet} in quantities sufficient for these studies and circumvent issues with obtaining mitotic, SAC-active cells upon ectopic expression of p31^{Comet}, we phosphorylated recombinant p31^{Comet} in mitotic extracts. Recombinant GST-p31^{Comet} was incubated in SAC-active or SAC-inactive extracts, purified, and resolved on Phos-tag gels to facilitate analysis of the phosphorylated protein (Fig. 5*A*). Mass spectrometry analysis of phosphorylated p31^{Comet} band identified phosphorylation of Ser-102 in the slower migrating band, whereas the unmodified peptide was identified in the lower, faster migrating band (Fig. 5, *B* and *C*).

p31^{Comet} Ser-102 Phosphorylation Status Modulates SAC Activity in Vivo—Phosphorylation of p31^{Comet} Ser-102 is a strong candidate for modulating p31^{Comet}-Mad2 binding. Ser-102 lies in a flexible loop adjacent to the Mad2-interacting residue Gln-83 and is thus physically poised to regulate this interaction (18). To examine the importance of Ser-102 phosphorylation *in vivo*, we constructed isogenic HeLa cells harboring tetracycline-inducible wild type p31^{Comet} or the S102A mutant (Fig. 6*A*). We first tested whether phosphorylation of Ser-102 is required for the decreased electrophoretic mobility we observed for endogenous p31^{Comet} in mitosis (Fig. 4*C*). Overexpression of p31^{Comet} abrogates Mad2-dependent mitotic arrest. To facilitate the accumulation of exogenous p31^{Comet}-expressing cells in mitosis that is required for analyzing phosphorylation in intact cells, we induced p31^{Comet} proteins in cells overexpressing Mad2 to buffer the effects of increased p31^{Comet} levels and then treated the cells with nocodazole. Mutation of Ser-102 prevented the mitotic phosphorylation shift of p31^{Comet} (Fig. 6*B*).

In conjunction with our data above, these results suggest that phosphorylation of Ser-102 alters the affinity of p31^{Comet} for Mad2 in mitosis. Thus, we postulated that the increased affinity

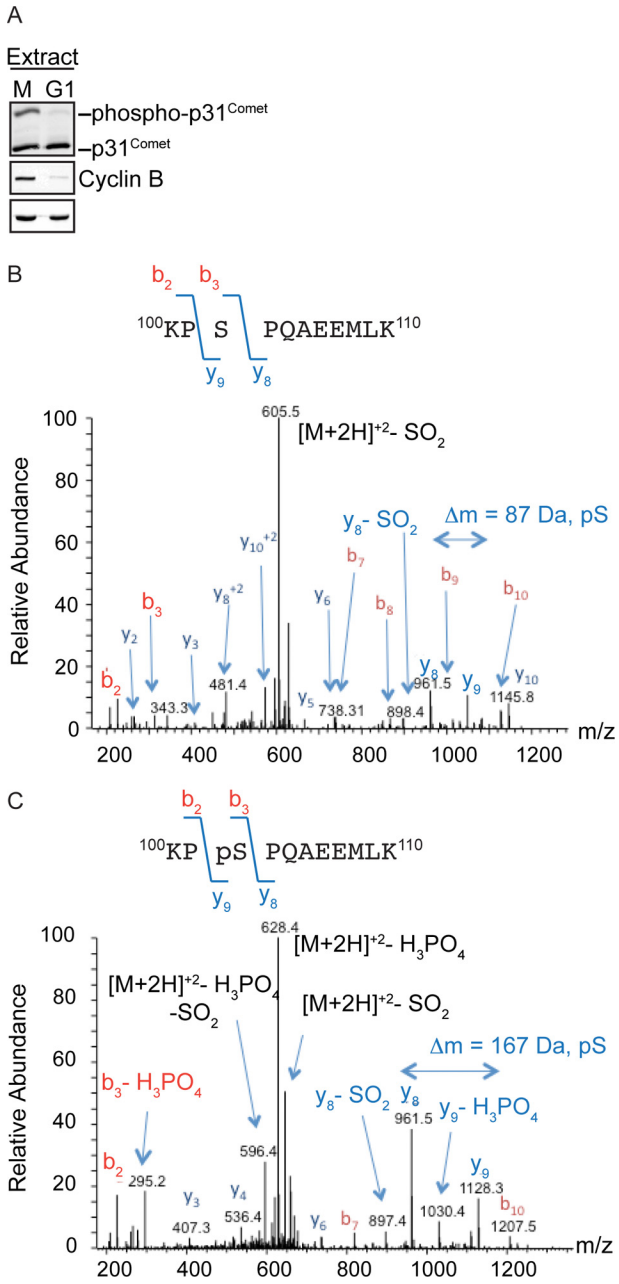

FIGURE 5. **p31^{Comet} Ser-102 is phosphorylated in mitosis.** *A*, recombinant p31^{Comet} was incubated in mitotic (*M*) or G_1 extracts and resolved by Phos-tag SDS-PAGE. Cyclin B levels were monitored to confirm the mitotic status of the extract. *B* and *C*, LC-MS/MS analysis of the p31^{Comet} tryptic digests from *A* identified the ^{100}KPSPQAEEMoLK^{110} peptide in both the unmodified and Ser-102 phosphorylated forms. The CID spectra for the unmodified peptide (*B*) contains several sequence-specific ions, including the y9 and y8 ions whose mass difference is 87 Da, consistent with an unmodified Ser residue. Although the CID spectra of the modified peptide (*C*) looks similar to the unmodified form, there are several differences including the presence of several H_3PO_4 neutral loss peaks, and the mass difference between y9 and y8 ions is 167 Da, consistent with Ser-102 as the site of phosphorylation.

of p31^{Comet} S102A for Mad2 would enhance its ability to silence the SAC. We tested the ability of exogenous p31^{Comet} in these cells to silence nocodazole-induced activation of the SAC in asynchronous cells. These analyses revealed a modest increase in SAC silencing by the p31^{Comet} S102A relative to wild type-expressing cells (data not shown). We repeated these analyses in synchronized cells. p31^{Comet} expression was induced (or not) upon release from a thymidine block. Cells were then challenged with nocodazole and the mitotic index was determined. Whereas control cells efficiently accumulated in mitosis, expression of exogenous p31^{Comet} proteins resulted in a dramatic decrease in the mitotic index. Importantly, expression of S102A produced a significantly stronger bypass of SAC activity in comparison with wild type (Fig. 6*C*).

Our experiments thus far indicate that phosphorylation of Ser-102 does play a role in diminishing the antagonism of Mad2 by p31^{Comet} during mitosis. Because phosphorylated p31^{Comet} still binds Mad2, overexpression of these proteins should bypass Mad2-mediated arrests, as has been shown for overexpression of wild type p31^{Comet}. Under these conditions, a single time point may not be sufficient to fully reveal the importance of phosphorylating Ser-102. We thus repeated the experiments above and monitored the duration of mitotic arrest in induced or uninduced cells in real time. Consistent with our above results, these analyses confirmed that exogenous p31^{Comet} proteins are capable of bypassing Mad2-mediated arrest. However, analysis of mitotic duration revealed that failure to phosphorylate Ser-102 enhances the ability of p31^{Comet} to silence SAC activity (Fig. 6, *D* and *E*). Together, our results indicate that phosphorylation of p31^{Comet} Ser-102 is an important event in the regulation of Mad2 activity *in vivo*.

DISCUSSION

Recent studies from a number of laboratories have highlighted the importance of mechanisms that promote recovery from the activation of the SAC, which occurs in every cell cycle. Although several proteins and events have been shown to promote recovery from SAC-mediated mitotic arrest, the regulation of these processes is unknown. p31^{Comet} is the best characterized component of the SAC recovery machinery (12–16). p31^{Comet} is required for efficient progression beyond metaphase and timely resumption of mitotic progression upon release from spindle poisons such as nocodazole.

Recovery from SAC activity requires two steps: 1) termination of SAC signaling and MCC formation and 2) disassembly of preexisting MCCs. p31^{Comet} specifically binds C-Mad2 via the same binding interface as O-Mad2 (9, 12, 17, 18). p31^{Comet} silences SAC activity *in vitro* and *in vivo* in a manner that requires this interaction with Mad2 (18). p31^{Comet} interacts with C-Mad2 in both the MCC and the C-Mad2·Mad1 complex, and it has been suggested that it may participate in both steps of SAC inactivation (9, 12, 17–19). However, it is currently unclear which step p31^{Comet} participates in *in vivo* as evidence for and against both models has been presented.

p31^{Comet} is coordinately expressed with Mad2 during the cell cycle.[3] Whereas Mad2 is required in early mitosis, p31^{Comet} is required for efficient progression beyond metaphase, suggesting that it becomes active to inhibit Mad2 at this point. Consistent with this idea, APC^{Cdc20} remains inhibited in extracts derived from cells arrested in prometaphase by nocodazole treatment, despite the presence of p31^{Comet}. We have shown

[3] Date, D. A., Burrows, A. C., and Summers, M. K. (2013) Coordinated regulation of p31^{Comet} and Mad2 expression is required for cellular proliferation. *Cell Cycle* **12,** 3824–3832.

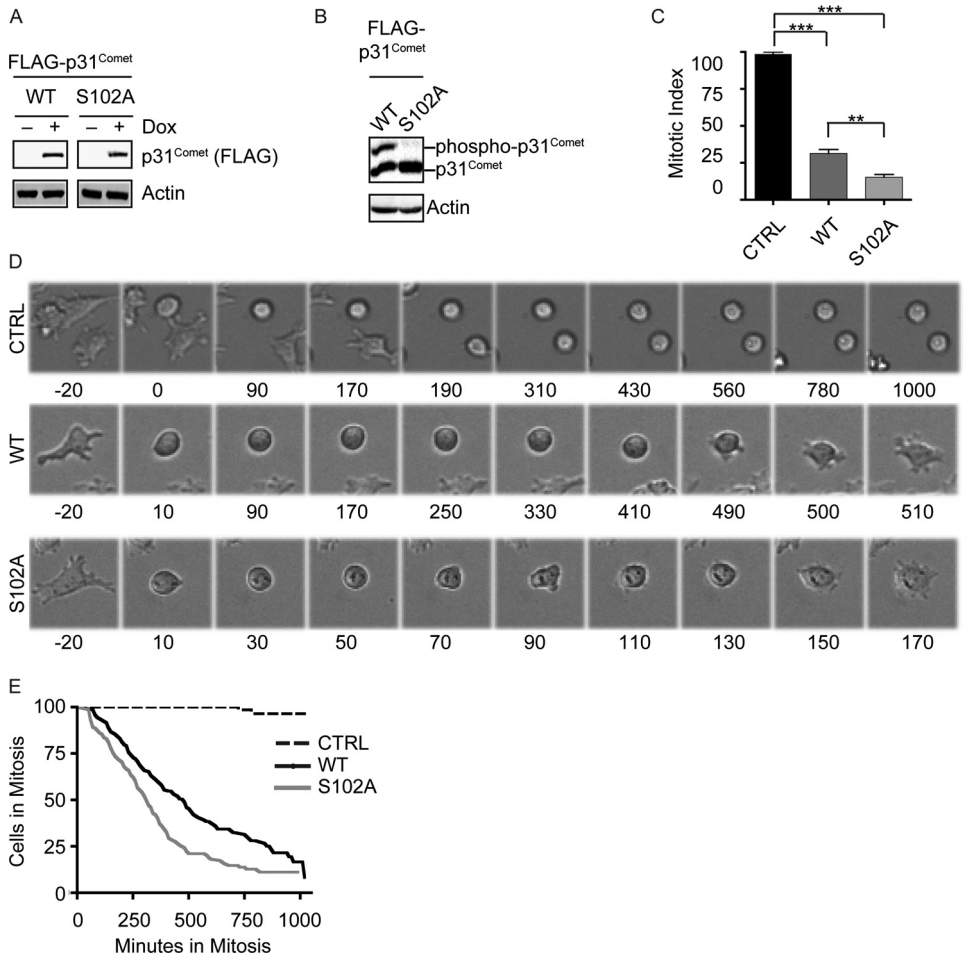

FIGURE 6. **Phosphorylation of Ser-102 attenuates the antagonism of Mad2 by p31^{Comet} *in vivo*.** *A*, expression of p31^{Comet} wild type (WT) or S102A mutant proteins was induced with doxycycline (*Dox*) in isogenic HeLa cell populations. *B*, cells from *A* were transfected with Mad2-encoding constructs and arrested in mitosis by a thymidine-nocodazole protocol. Mitotic cells were collected by shake-off and exogenous p31^{Comet} proteins were analyzed by Phos-tag SDS-PAGE and probed for the FLAG epitope. *C*, cells were treated as described in *B*, and mitotic index was determined. The mitotic index of uninduced cells was set at 100%. *Error bars* represent S.D. ($n = 3$). **, $p < 0.01$; ***, $p < 0.001$. *D* and *E*, cells were synchronized by thymidine-nocodazole block. Mitotic duration was analyzed by time-lapse microscopy. *D*, representative images of mitotic progression in the indicated cell populations. The time (in min) relative to mitotic entry is indicated. *E*, plot showing the cumulative number of cells in mitosis at the indicated times for each cell population. *CTRL*, control.

that this inhibition is mediated by the MCC, suggesting that p31^{Comet} is not active in prometaphase (20). However, p31^{Comet} interacts with Mad2 throughout the cell cycle. We show that this binding reflects inhibition of Mad2. Thus, regardless of which step(s) of SAC silencing p31^{Comet} promotes, how the SAC is activated despite inhibition of Mad2, is a critical question.

We have determined that although the interaction of p31^{Comet} with Mad2 is readily detectable when the SAC is active, the binding between these two proteins is weakened in these cells. Phosphorylation of p31^{Comet} mediates this weakened interaction. Specifically, we identified phosphorylation of Ser-102 in the mitosis-specific phosphorylated form of p31^{Comet}. Ser-102 is positioned near a key residue, Gln-83, in the p31^{Comet}-Mad2 interaction. To address the impact of phosphorylating p31^{Comet} Ser-102 on its interaction with Mad2, we utilized competitive binding assays *in vitro*. These analyses revealed that phosphorylation of Ser-102 is sufficient for inducing a subtle but significant weakening of the binding of p31^{Comet} and Mad2 *in vitro*. Importantly, preventing phosphorylation of Ser-102 enhances the ability of exogenous p31^{Comet} to antagonize Mad2 *in vivo*. Given the dynamic nature of SAC activation *in vivo* (13, 19, 21) and the potential involvement of other factors and modifications (*e.g.* Mad2 phosphorylation) in attenuating the p31^{Comet}-Mad2 interaction, it is likely that our *in vitro* assay may not fully recapitulate the impact of phosphorylating p31^{Comet} on Mad2 activation in an intact mitotic cell. Together, our data suggest a model of SAC regulation based on modulating the strength of the interaction of p31^{Comet} with Mad2. Although our data strongly support Ser-102 as a key regulatory site, we note that this residue, as with many reported phosphosites in human p31^{Comet}, is not highly conserved in p31^{Comet} from other species. However, we note that these loop regions generally contain potential phosphosites, suggesting that the mechanism is conserved.

Attenuating the interaction of p31^{Comet} with C-Mad2 would enhance the ability of O-Mad2 and/or BubR1 to compete with p31^{Comet} for binding to C-Mad2 at the kinetochore or in the MCC, respectively, promoting SAC activity (15, 16, 18, 26). Additionally, attenuating constant inhibition of C-Mad2, rather than activating inhibition of Mad2 at metaphase, would ensure rapid APC^{Cdc20} activation and progression from meta-

phase to anaphase upon satisfaction of the SAC. However, our analyses indicate that the entire pool of p31^{Comet} is not phosphorylated during mitosis, even in nocodazole-treated cells in which the SAC is maximally active. This finding is in line with data showing that p31^{Comet} functions during prometaphase to prevent maximal SAC activation (19). In addition, these findings suggest that antagonistic kinase and phosphatase activities are required for regulation of p31^{Comet} in mitosis. It will be important to identify these enzymes to fully understand the importance of this p31^{Comet} phosphoregulation. Future studies will pursue these enzymes and compare the interplay of p31^{Comet} phosphorylation with additional events, including phosphorylation of critical interacting proteins such as Mad2 or Cdc20, which are known to contribute to regulation of the SAC (27, 28).

Acknowledgments—We thank Dr. Monica Venere for assistance with live cell imaging, helpful discussions, and critical reading of the manuscript and Dr. Belinda Willard for mass spectrometry analysis.

REFERENCES

1. Sudakin, V., Chan, G. K., and Yen, T. J. (2001) Checkpoint inhibition of the APC/C in HeLa cells is mediated by a complex of BUBR1, BUB3, CDC20, and MAD2. *J. Cell Biol.* **154,** 925–936
2. Luo, X., Tang, Z., Xia, G., Wassmann, K., Matsumoto, T., Rizo, J., and Yu, H. (2004) The Mad2 spindle checkpoint protein has two distinct natively folded states. *Nat. Struct. Mol. Biol.* **11,** 338–345
3. Luo, X., Fang, G., Coldiron, M., Lin, Y., Yu, H., Kirschner, M. W., and Wagner, G. (2000) Structure of the Mad2 spindle assembly checkpoint protein and its interaction with Cdc20. *Nat Struct Biol* **7,** 224–229
4. Luo, X., Tang, Z., Rizo, J., and Yu, H. (2002) The Mad2 spindle checkpoint protein undergoes similar major conformational changes upon binding to either Mad1 or Cdc20. *Mol Cell* **9,** 59–71
5. Sironi, L., Melixetian, M., Faretta, M., Prosperini, E., Helin, K., and Musacchio A. (2001) Mad2 binding to Mad1 and Cdc20, rather than oligomerization, is required for the spindle checkpoint. *EMBO J.* **20,** 6371–6382
6. Sironi, L., Mapelli, M., Knapp, S., De Antoni, A., Jeang, K. T., and Musacchio, A. (2002) Crystal structure of the tetrameric Mad1-Mad2 core complex: implications of a 'safety belt' binding mechanism for the spindle checkpoint. *EMBO J.* **21,** 2496–2506
7. De Antoni, A., Pearson, C. G., Cimini, D., Canman, J. C., Sala, V., Nezi, L., Mapelli, M., Sironi, L., Faretta, M., Salmon, E. D., and Musacchio, A. (2005) The Mad1/Mad2 complex as a template for Mad2 activation in the spindle assembly checkpoint. *Curr. Biol.* **15,** 214–225
8. Nezi, L., Rancati, G., De Antoni, A., Pasqualato, S., Piatti, S., and Musacchio, A. (2006) Accumulation of Mad2-Cdc20 complex during spindle checkpoint activation requires binding of open and closed conformers of Mad2 in *Saccharomyces cerevisiae*. *J. Cell Biol.* **174,** 39–51
9. Mapelli, M., Massimiliano, L., Santaguida, S., and Musacchio, A. (2007) The Mad2 conformational dimer: structure and implications for the spindle assembly checkpoint. *Cell* **131,** 730–743
10. Mariani, L., Chiroli, E., Nezi, L., Muller, H., Piatti, S., Musacchio, A., and Ciliberto, A. (2012) Role of the Mad2 dimerization interface in the spindle assembly checkpoint independent of kinetochores. *Curr. Biol.* **22,** 1900–1908
11. Kulukian, A., Han, J. S., and Cleveland, D. W. (2009) Unattached kinetochores catalyze production of an anaphase inhibitor that requires a Mad2 template to prime Cdc20 for BubR1 binding. *Dev. Cell* **16,** 105–117
12. Xia, G., Luo, X., Habu, T., Rizo, J., Matsumoto, T., and Yu, H. (2004) Conformation-specific binding of p31(comet) antagonizes the function of Mad2 in the spindle checkpoint. *EMBO J.* **23,** 3133–3143
13. Jia, L., Li, B., Warrington, R. T., Hao, X., Wang, S., and Yu, H. (2011) Defining pathways of spindle checkpoint silencing: functional redundancy between Cdc20 ubiquitination and p31(comet). *Mol. Biol. Cell* **22,** 4227–4235
14. Hagan, R. S., Manak, M. S., Buch, H. K., Meier, M. G., Meraldi, P., Shah, J. V., and Sorger, P. K. (2011) p31comet acts to ensure timely spindle checkpoint silencing subsequent to kinetochore attachment. *Mol. Biol. Cell* **22,** 4236–4246
15. Westhorpe, F. G., Tighe, A., Lara-Gonzalez, P., and Taylor, S. S. (2011) p31comet-mediated extraction of Mad2 from the MCC promotes efficient mitotic exit. *J. Cell Sci.* **124,** 3905–3916
16. Fava, L. L., Kaulich, M., Nigg, E. A., and Santamaria, A. (2011) Probing the *in vivo* function of Mad1:C-Mad2 in the spindle assembly checkpoint. *EMBO J.* **30,** 3322–3336
17. Mapelli, M., Filipp, F. V., Rancati, G., Massimiliano, L., Nezi, L., Stier, G., Hagan, R. S., Confalonieri, S., Piatti, S., Sattler, M., and Musacchio, A. (2006) Determinants of conformational dimerization of Mad2 and its inhibition by p31comet. *EMBO J.* **25,** 1273–1284
18. Yang, M., Li, B., Tomchick, D. R., Machius, M., Rizo, J., Yu, H., and Luo, X. (2007) p31comet blocks Mad2 activation through structural mimicry. *Cell* **131,** 744–755
19. Varetti, G., Guida, C., Santaguida, S., Chiroli, E., and Musacchio, A. (2011) Homeostatic control of mitotic arrest. *Mol. Cell* **44,** 710–720
20. Summers, M. K., Pan, B., Mukhyala, K., and Jackson, P. K. (2008) The unique N terminus of the UbcH10 E2 enzyme controls the threshold for APC activation and enhances checkpoint regulation of the APC. *Mol. Cell* **31,** 544–556
21. Reddy, S. K., Rape, M., Margansky, W. A., and Kirschner, M. W. (2007) Ubiquitination by the anaphase-promoting complex drives spindle checkpoint inactivation. *Nature* **446,** 921–925
22. Miniowitz-Shemtov, S., Teichner, A., Sitry-Shevah, D., and Hershko, A. (2010) ATP is required for the release of the anaphase-promoting complex/cyclosome from inhibition by the mitotic checkpoint. *Proc. Natl. Acad. Sci. U.S.A.* **107,** 5351–5356
23. Teichner, A., Eytan, E., Sitry-Shevah, D., Miniowitz-Shemtov, S., Dumin, E., Gromis, J., and Hershko, A. (2011) p31comet Promotes disassembly of the mitotic checkpoint complex in an ATP-dependent process. *Proc. Natl. Acad. Sci. U.S.A.* **108,** 3187–3192
24. Torres, J. Z., Miller, J. J., and Jackson, P. K. (2009) High-throughput generation of tagged stable cell lines for proteomic analysis. *Proteomics* **9,** 2888–2891
25. Kinoshita, E., Kinoshita-Kikuta, E., Takiyama, K., and Koike, T. (2006) Phosphate-binding tag, a new tool to visualize phosphorylated proteins. *Mol. Cell Proteomics* **5,** 749–757
26. Tipton, A. R., Wang, K., Link, L., Bellizzi, J. J., Huang, H., Yen, T., and Liu, S. T. (2011) BUBR1 and closed MAD2 (C-MAD2) interact directly to assemble a functional mitotic checkpoint complex. *J. Biol. Chem.* **286,** 21173–21179
27. Miniowitz-Shemtov, S., Eytan, E., Ganoth, D., Sitry-Shevah, D., Dumin, E., and Hershko, A. (2012) Role of phosphorylation of Cdc20 in p31(comet)-stimulated disassembly of the mitotic checkpoint complex. *Proc. Natl. Acad. Sci. U.S.A.* **109,** 8056–8060
28. Kim, S., Sun, H., Ball, H. L., Wassmann, K., Luo, X., and Yu, H. (2010) Phosphorylation of the spindle checkpoint protein Mad2 regulates its conformational transition. *Proc. Natl. Acad. Sci. U.S.A.* **107,** 19772–19777